Some Tsunami Characteristics Deducible from Tide Records

W. G. VAN DORN

Scripps Institution of Oceanography, University of California, San Diego, La Jolla, CA 92093

(Manuscript received 5 July 1983, in final form 23 November 1983)

ABSTRACT

After an initial 40-hour "diffusion" period, the time decay of tsunami variance was found to be uniformly exponential for 28 events among eight Pacific tide stations. These results essentially confirm Munk's acoustic decay hypothesis except that the decay (*e*-folding) time (22 h) more nearly equaled the ocean's normal mode transit time (21 h) than Munk's mean collision time (14 h).

Relative tsunami energy, obtained by extrapolating exponential decay back to $t = 0$, was found to be similarly ranked among tsunamis at all stations and roughly proportional to seismic energy. A total energy estimate for the tsunami of 9 March 1957, obtained by correcting the observed energy decay at Wake Island for instrument and island response, provided normalized total energy estimates for all tsunamis that were consistent with independent estimates by Kajiura and by Aida.

Similarities between power spectra computed from these time series suggests that station response is primarily linear normal-mode forcing of the continental shelves by the isotropic tsunami spectrum in deep water, rather than resonant excitation of trapped edge waves on the shelves.

1. Introduction

Munk (1963) was the first to note that tsunami energy in the sea appears to decay in much the same manner as sound intensity does in a closed room, based on the comparison of consecutive spectra computed for the Chilean tsunami of 22 May 1960 (Miller *et al.*, 1962). Being interested, at the time, in the absorption of tidal energy, which he felt might occur through some common process, Munk developed an "acoustic analog" decay model for the ocean and examined a variety of decay mechanisms. In brief, he concluded that:

- A tsunami is probably well diffused over the Pacific after one or two transoceanic reflections (14–28 h),
- It thereafter loses energy—principally by absorption during multiple coastal reflections—at a rate of about e^{-1} per reflection, relatively insensitive to frequency,
- Approximately 13% of its energy leaks into other oceans through "windows" around Antarctica,
- "Diffusion" needs to be better defined and the physical mechanism of absorption remains obscure.

In this paper, the problem of tsunami energy decay is reexamined in a somewhat different context. It was hypothesized that, if the initial tsunami impulse were indeed diffused to the point of isotropy in a time short compared to the ocean's reverberation time, then thereafter, all oceanic tidegages should be exposed to the same nondirectional energy spectrum across their respective shelf margins and meaningful comparisons between relative tidegage responses might be possible. As shown below, this hypothesis is amply verified.

2. Data acquisition and processing

a. Procurement

All tide data for this study were obtained from U.S. Standard gage records, circa 1965 and before (Schoreman, 1941).[1] Frequency response of the standard gage is well-known (Cross, 1968) and can be considered linear only for waves of amplitude $a < a_0(f/f_0)^2$, where $a_0 = 1000$ cm and $f_0 = 1$ cycle per hour (cph). Because interest was attached principally to the reverberatory phase, data were restricted to the five largest tsunamis of this century, which will be referred to hereinafter only by year. From more than one hundred 35-millimeter film strips reviewed at World Data Center A, 28 station-events were selected, comprising sets of 2–5 tsunamis at each of eight tide stations (Table 1). Selection criteria included geographical distribution (Fig. 1), record quality and evidence of activity distinguishable above background for at least 100 hours. The tsunamis originated from all recent centers of tectonic activity in the Pacific, while the tide stations effectively blanket the northeast quadrant of the Pacific.

The original tide records containing these events were requested from the National Weather Service ar-

[1] Since 1965, the U.S. has replaced all tidegages with new instruments that record an instantaneous level every six minutes on punched paper tape. Such data are useless for analysis of tsunamis.

TABLE 1. Energy index E_0 (cm^2) for 28 tsunami-station combinations.

Tsunami location	1 Apr 1946 Aleutians	4 Nov 1952 Kamchatka	9 Mar 1957 Aleutians	22 May 1960 Chile	28 Mar 1964 Alaska
Attu			160	5400	990
Unalaska			52	1500	
Crescent City		2800		10 000	
San Francisco	40		54	1200	350
San Diego	85	640	150	2400	450
Honolulu	68	630	90	1800	150
Hilo		680	200	2000	550
Pago Pago		340		1000	180

chives and six-day sections including the tsunami and 24 hours of preceding background were copied on velum in a continuous flow xerox machine of the type used for large engineering drawings.

b. Digitizing

The 28 records were divided by vertical lines into 12-h sections and table-digitized with a hand-moved cursor onto magnetic tape at a constant data rate of 120 samples per second. The data segments were then linked together and linearly interpolated to give continuous time series with a uniform data density of 100 points per hour. The quality tests applied to these series were that computer printouts to the same scale as the originals could be overlaid thereon without significant discrepancy and that the variance of 12-hour sections digitized by two or more persons did not differ by more than 2 db. Despite these controls, several original records exhibited a low-amplitude fine structure that could not be resolved in digitizing. In such cases the operator attempted to follow the center of the fuzzy trace, with some undetermined loss of high-frequency energy. The *variance,* however, could be estimated from the trace width, and was always 30–40 db below that of signals of interest to this discussion.

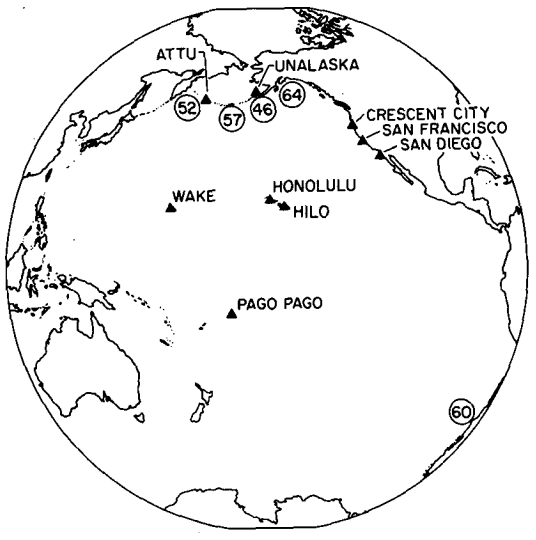

FIG. 1. Distribution of tsunami epicenters (circles) and tide stations (triangles) covering the northeast Pacific.

c. Prefiltering

After amplitude correction to uniform scale, all time series were high-passed to remove tidal components, using a numerical, zero-phase shift filter having a 40 db attenuation within a 0.5 cph bandwidth, centered on 0.375 cph.

d. Spectra

All time series were subdivided into 800-point (8 h) segments, filtered with a 250-weight Hanning taper to suppress aliasing. Power spectral energy density was computed for 50 frequency bands and averaged to yield 26 spectral estimates at frequency intervals of two cycles per hour (2 cph), with 95% confidence limits of approximately ±1.8 db.

Reference is also made herein to a data series obtained for the tsunami of 9 March 1957 from a special recording station at Wake Island (Van Dorn, 1963). For this study, the series was reexamined, several instrumental "glitches" were excised and patched over from adjacent sections and file gaps were completed by insertion of missing data supplied by Royer and Reid (1971). The completed series, consisting of 13 400 points, read at 120 points per hour, was high-passed as above, and subdivided into 1200-point (10-h) segments. Spectra from these segments were computed in 60 bands, averaged to give 31 estimates at 2 cph intervals, with 95% confidence limits of approximately ±1.5 db. These estimates were then further corrected for instrument and island response, as described in the Appendix to this paper.

3. General decay law

To test Munk's hypothesis of the early diffusion of directive energy flux into longer-term, isotropic, reverberatory decay, all tidegage time series were divided into 12-h segments (1200 data points), beginning 12 h before the first tsunami arrival, and the variance was computed for each segment. For each tide station, a

semilogarithmic plot was constructed showing the decay of variance (energy) with time after earthquake occurrence for each tsunami recorded there.

Figure 2 is a representative station plot for three tsunamis at Massacre Bay, Attu, Aleutian Islands. In all three cases, a least-squares fit to the variances for times longer than ~40 hours are lines with nearly the same slope. This was also found to be true for all other station events. Specifically, the mean e-folding (decay) time for all tsunamis at one station and its converse agree within 0.1% of the value $t_0 = 22.0 \pm 0.07$ h. Evidently all tsunamis obey the common decay law

$$E_0(t) = E_0 \exp(-t/t_0), \quad t > 40 \text{ h}, \qquad (1)$$

where E_0 can be regarded as a tsunami energy index, modified by local station response. Values of E_0 for all station-events are listed in Table 1. The decay lines in Fig. 2 satisfy (1) and were drawn to pass through the centroid of their respective reverberatory datasets.

This result confirms Munk's acoustic model, although both diffusion time (40 h) and decay time (22 h) are about 50% longer than he proposed on the basis of limited data. Tsunami energy appears to be well diffused after three mean (2 maximum) reflection times and thereafter, to decay at a rate of about 50% per mean reflection (14 h). Further evidence that this decay is insensitive to frequency is given in Section 7.

Two further comments concerning the decay of variance deserve mention.

Munk (1963) concluded that the principal mechanism for diffusion was scattering from coastlines and islands, for which he expected the scattered signal to decay as t^{-2} and t^{-1} respectively. His models were necessarily simple and not directly applicable to tsunamis originating at the coastline. However, from present data the following pertain:

1) Diffusive decay at island stations generally commences with a high value and decays roughly as t^{-1} to tangency with the equilibrium (reverberatory) decay line.

2) Diffusion appears to be completed more rapidly at islands than at continental shorelines, sometimes as early as 30 h after tsunami generation.

3) In large coastal harbors (San Francisco and San Diego) the diffused variance commences low and approaches the equilibrium decay line from beneath. This behavior is characteristic of overdamped response of a resonant system, but the physical process remains obscure.

4) Among the five events examined, the 1964 tsunami was singular for its long and erratic diffusion history, persisting, even during reverberation, as large deviations from the decay line. Physically this tsunami was characterized by its mode of generation in shallow water as a single broad intumescence (Van Dorn, 1972). The absence of high-frequency components, that are more easily scattered, in Munk's analysis, might explain its slow diffusion.

With regard to reverberatory decay, the deviation of 12-hourly variance from the equilibrium decay lines can be taken as a measure of the degree of isotropy attained by the ocean. The statistics of deviations relevant to the energy indices in Table 1 are given in Table 2, from which it is apparent that: the north Pacific is indeed remarkably isotropic after 40 hours; with regard to tsunamis the 1964 event had the largest deviations and of the stations, Pago Pago. But the fact that the mean, largest and smallest deviations are nearly the same among stations and tsunamis suggests that the deviations are more likely random than the result of some specific topographically or frequency selective process. Because all present data is from the northeast Pacific, it would be desirable to examine energy decay for these same tsunamis in, say, Japan, Chile and New Zealand.

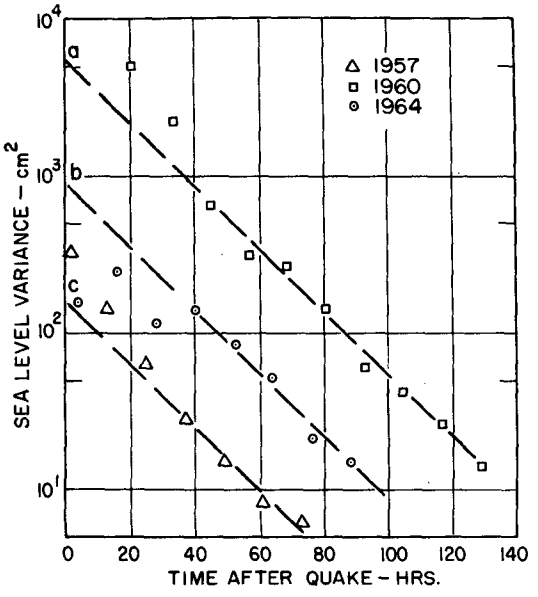

FIG. 2. Decay of variance for three tsunamis at Attu, Aleutian Islands.

4. Relative tsunami energy

The general decay law (1) implies that, during reverberative decay, total tidegage energy within the tsunami band is everywhere in equilibrium with the ocean, and that for any tsunami, differences in the energy indices E_0 between tide stations are attributable only to local response factors. Additionally, the ratio of two tsunami indices recorded at the same tide station should reflect their relative energies, modified only by spectral differences. But if tsunami spectra are not too dissimilar and station responses are relatively insensitive to frequency, then one might reasonably estimate

TABLE 2. Mean deviations (db) from energy indices in Table 1.

	Mean	Largest	Smallest
All tsunamis at one station	(all) 2.6	(Pago Pago) 4.2	(Attu) 1.8
One tsunami at all stations	(all) 2.8	(1964) 3.7	(1946) 2.0

the relative energies of tsunamis by comparing their respective energy indices.

Figure 3 is the simplest comparison. The values of E_0 for all five tsunamis have been plotted as regression lines normalized to the 1960 tsunami indices at all common recording stations. Noting that the data deviations from their respective regression lines are generally smaller than the line separations, we conclude that tsunamis can indeed be ranked according to relative energy, despite the wide variations in individual response evident in Table 1. The best estimates of relative energy, obtained from intercepts of the regression lines with the top axis of Fig. 3, are listed at the top of the figure as percentages of 1960 energy.

This representation somewhat reorders the prevailing view of relative energy. While the Chilean tsunami of 1960 is everywhere recognized as the largest event of this century, from the standpoint of coastal effects the Alaskan tsunami of 1964 is generally considered to have been more damaging than the Kamchatka tsunami of 1952. Yet, Fig. 3 clearly shows that the latter was nearly twice as energetic. The Aleutian tsunamis of 1957 and 1946, both of which caused considerable damage and had similar run-up statistics in Hawaii (Van Dorn, 1965), are here rated nearly equal in energy, yet both had less than 5% of that of the 1960 tsunami.

Deviations from the regression lines in Fig. 3 are most probably due to variations in spectra between tsunamis and responses between stations, with low values implying impedance mismatch and high values, resonant amplification. Among tsunamis, the largest deviations apply, again, to 1964, mentioned in Section 3 as having a spectrum nearly devoid of high frequencies, and to 1957, which will be discussed in Section 6 as resulting from a complex multiple-source, peaked at relatively high frequency. Among stations, the greatest deviations—Hilo (1957), a low value and Honolulu (1964), a high value—both occurred in Hawaii. Neither has an obviously simple explanation.

Finally, we note in Fig. 3 that, with one exception (Unalaska), station energy among all tsunamis increased geographically northward from Pago Pago to Attu. The tide range in the northeast Pacific increases in much the same manner. Is this just an interesting coincidence?

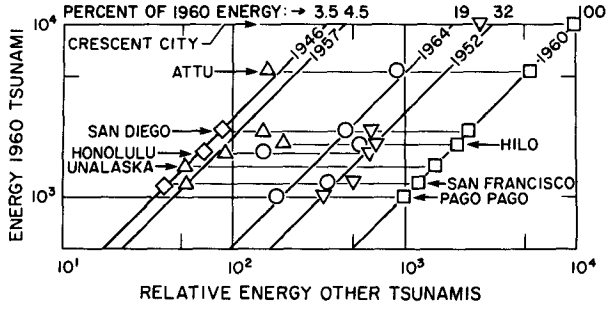

FIG. 3. Energy indices E_0 for 28 station events normalized to 1960 energy.

5. Relative seismic energy

The regular ranking of tsunami energies in Fig. 3 suggests comparison with relative seismic energies. Fig. 4 shows the appropriate regression, again normalized on Chile 1960. Seismic (Richter) magnitudes were similarly normalized and are listed in the data circles, which have diameters of ±0.1 Richter units.

Because of the complexity of seismic sources (Kajiura, 1981) no attempt is made here to compare Fig. 4 with many previous similar correlations. It suffices to say that, except for 1957, tsunami energy appears to be roughly proportional to seismic energy. The 1946 tsunami, always mysterious because of its low Richter magnitude and great damage in Hawaii, fits the regression line quite well; whereas the 1957 event had the same damage statistics and a much larger quake magnitude—a circumstance more easily explained.

6. Total tsunami energy

Kajiura (1981) has recently reviewed past estimates of total tsunami energy together with attempts to meaningfully relate them to earthquake source parameters. Regarding tsunamis, he concluded that the numerical inversion method of Aida (1978) provides the most reliable energy estimates. Kajiura himself proposed a new earthquake fault model relating tsunami

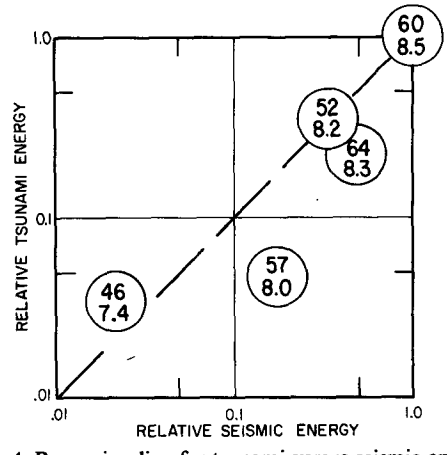

FIG. 4. Regression line for tsunami versus seismic energy.

energy E_t to the moment-magnitude M_w of an earthquake:

$$\log E_t[\text{ergs}] = 2M_w + \log F + 5.5, \quad (2)$$

where $0.01 < F < 0.1$ is a function of fault parameters whose maximum value gives a reasonable upper bound to Aida's estimates for 13 tsunamis originating near Japan. In (2), M_w is also a geophysical parameter related to seismic moment M_0 by

$$M_w = (\log M_0 - 16.5)/1.5. \quad (3)$$

Seismic moment M_0 has been evaluated by Ohnaka (1978) for three of the earthquakes considered here (1952, 1960, 1964), which provides a basis for an independent energy comparison with present results.

The best independent estimate of total tsunami energy, of course, would be that obtained from the reverberatory decay of a tsunami recorded in mid-ocean. There being no record, the best alternative is that of the 1957 tsunami obtained by Van Dorn (1963) from a special instrument station on Wake Island. In principal, for linear interactions the influence of the island on the (isotropic) wave field can be removed by dividing the reverberative spectrum by the appropriate frequency-response operator. (Van Dorn's 1963 estimates of decay rate and total energy were in error, owing to failure to correct for island response.) The details of this tedious procedure are given in the Appendix.

Figure 5 shows the relevant frequency-dependent corrections for instrument prefiltering and island response. By coincidence rare in geophysics, the two corrections almost cancel. For practical purposes, decay spectra computed for the 1957 tsunami at Wake can be taken as if the island did not exist, and the variances can be calculated directly from the original data. Fig. 6 is a semilogarithmic plot of 12-hour variances against time. Their least-squares fit to the 22-hour decay line has a quake-time intercept, $E_0 = 5.0$ cm^2. The best estimate of total energy for the 1957 tsunami then is

$$E_t = pgE_0A = 9.0 \times 10^{21} \text{ ergs} \pm 1.6 \text{ db}, \quad (4)$$

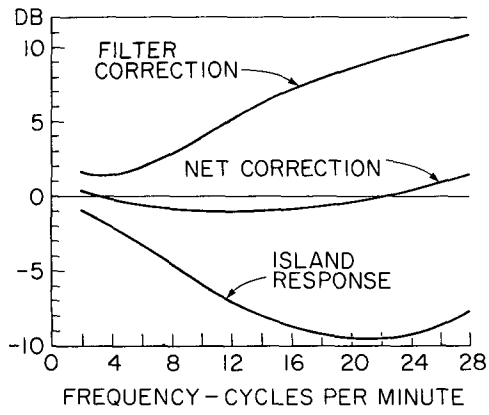

FIG. 5. Corrections to the 1957 tsunami record at Wake Island.

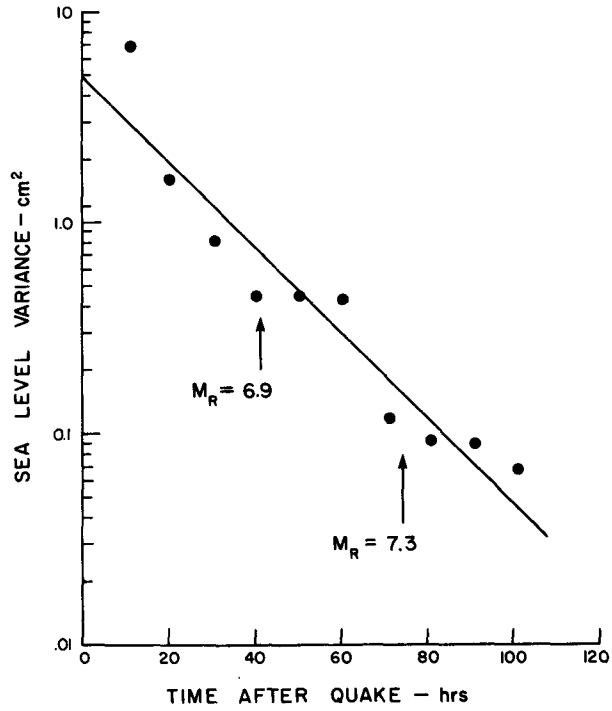

FIG. 6. Decay of variance at Wake Island for the tsunami of 9 March 1957.

where $A = 1.8 \times 10^{18}$ cm^2 is the area of the Pacific Ocean. The relative energies in Fig. 3 can now be normalized to (4) to give estimates of total energy for all five tsunamis, together with their standard deviations. The values are listed in Table 3, which also includes the three earthquake moments M_0, determined by Ohnaka (1978), and their respective moment magnitudes M_w computed from (3).

The comparison of present results with Kajiura's fault model and Aida's numerical inversion data is shown in Fig. 7. The solid line is Kajiura's upper bound for tsunami energy, assuming $F = 0.11$. The close agreement supports the three independent methods of estimating tsunami energy.

The accuracy of the above energy estimates depends upon the best fit of the decay line in Fig. 6 to the reverberative ($t > 40$ h) data distribution, which, in fact, appears to be more steplike than linear. One ex-

TABLE 3. Total energy estimates for the tsunamis.

Tsunami	Total tsunami energy (ergs)	Standard deviation (db)	Earthquake moment M_0	Moment magnitude M_w
22 May 1960	2.0×10^{23}	reference	2.7×10^{30}	9.5
4 Nov 1952	6.4×10^{22}	1.3	1.5×10^{27}	8.7
28 Mar 1964	3.8×10^{22}	1.6	7.5×10^{29}	9.2
9 Mar 1957	9.0×10^{21}	1.6	—	—
1 Apr 1946	7.0×10^{21}	0.1	—	—

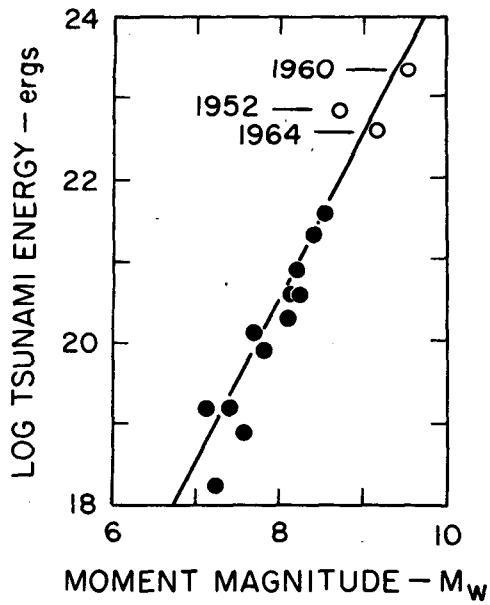

FIG. 7. Comparison of present total tsunami energy estimates (open circles) with Kajiura's fault model (diagonal line) and Aida's estimates for tsunamis near Japan (closed circles).

planation for this steplike decay has been suggested by Royer and Reid (1971), who identified several significant increases in spectral energy in this same data series with large earthquake aftershocks. Indeed, the two arrows in Fig. 6 give the Richter magnitudes and expected arrival times of wave energy at Wake for the two largest aftershocks, which can be seen to coincide quite well with steplike energy increases. Thus, the best interpretation of total energy for this tsunami might be as much as 20% larger than that indicated by the regression line. Perhaps significantly, these steps do not appear in the variance decay data at any tide station. The most likely explanation is that they represent early, coherent energy at Wake (the closest station), which becomes better diffused before reaching more distant stations.

The concept of the 1957 tsunami as a complex multiple source is further supported by Fig. 8, in which the time interval between consecutive wave crests (period) is plotted against time for the first 12 hours of the Wake record. The nine descending curves in this figure are dispersion curves, corresponding to the expected arrival times of wave energy from the initial shock and eight subsequent aftershocks obtained from the Earthquake Data Information Center, Boulder, Colorado. The data distribution clearly indicates that recurrences of low-frequency energy are consistent with at least four of these curves, although none but the initial shock has a magnitude listing. The irregularity of these recurrences precludes their being attributable to simple reflection from the Aleutian Island arc immediately north of the epicenter of this disturbance.

7. Spectra

a. Previous work

Of many tsunami spectral comparisons, only a few are relevant to reverberatory decay ($t > 40$ h). Miller *et al.* (1962) computed high resolution spectra for consecutive 40-hour record samples of the 1960 Chilean tsunami at La Jolla, noting that the spectra were remarkably similar, high frequencies decayed slightly faster than low frequencies and the decay rate did not vary much with time. From consecutive spectra of 8.3-hour record samples of three tsunamis recorded at tidegages in Honolulu and Hilo, Hawaii, Loomis (1966) concluded that time changes in spectra of a tsunami at a given station do not support any simple picture of a local response function and that comparative spectra for the same tsunami at these two stations were only coherent at low frequencies ($f < 6$ cph). Evidence of late stage spectral energy contributions from earthquake aftershocks has already been noted.

Because none of the spectra in the above studies exhibit features easily identifiable with local topography or tsunami characteristics, it was felt that lower resolution here might better reveal persistent trends among the various station-events for which data were available.

b. Wake Island

Reverberative spectra for the 1957 tsunami at Wake Island are of special interest because they represent the best estimate of the isotropic tsunami signature in deep water, to which coastal tidegages were simultaneously responding.

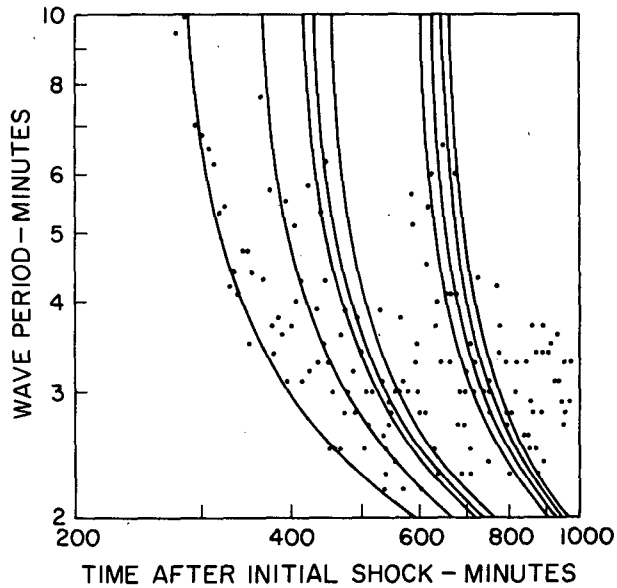

FIG. 8. Dispersion curves for early earthquake shocks and wave arrival times for the 9 March 1957 tsunami at Wake Island.

An interesting representation is that shown in Fig. 9, in which energy contours are mapped in frequency-time space. This plot was generated from the same high-passed data series used to compute the variances in Section 6, assuming that the corrections for instrument and island response cancel during isotropic decay. Because the latter correction is quite different at early times, when the tsunami flux is directional, this plot errs in underestimating the temporal energy density by ~5 db in the lower right corner. The error diminishes upwards and disappears after approximately 35 hours; it does not appreciably affect the following interpretation.

First, note that principal tsunami energy is peaked near the unusually high frequency of 14 cph and remains there with increasing time, as the tsunami is diffused towards isotropy. The two secondary tsunamis previously mentioned appear here as an island and plateau, centered at a much lower frequency (2 cph) and near 50 and 70 h, respectively, after tsunami arrival. Their energy contributions only alter the contour field by ~4 db, a relatively modest increase, considering that the principal energy peak stands ~28 db above background (38 db). From this picture, we can infer that the initial earthquake involved a relatively large displacement of a relatively small area (half-breadth ~ 50 km), whereas the secondary events comprised displacements about 16 times smaller over areas about 3 times as large.

For better comparison with tidegage results, Fig. 10 shows three conventional power spectra. At 2 cph per estimate, the resolution is about 70 times lower than that of Loomis (1966) and only features subtending more than 8 cph can be fully resolved. The upper curve refers to the first ten hours of the tsunami, when the energy flux—including scattered reflections from Japan to Alaska—can still be presumed quasi-directional. The middle curve applies to the period 40–50 h after tsunami arrival, when the flux is wholly isotropic. The plateau near the left margin corresponds to the island in the previous figure and represents the arrival of "new", directive energy from a large aftershock. Therefore, the isotropic spectrum from the initial shock more probably follows the dashed curve drawn about 4 db below the plateau. The lowest curve is background before the tsunami arrival. It is flat and nearly featureless within the 95% confidence limits of ±2 db. All three curves have been corrected for both instrument and island response.

The importance here of these results is twofold. First, the general congruence of the upper two curves suggests that, except for a 15 db energy reduction, there is very little change in the energy distribution among frequencies during diffusive decay. That is, energy attenuation by multiple reflection and scattering is not a frequency-selective process. Second, the flat background implies an absence of trapped modes so that small, isolated islands make satisfactory observation platforms for long waves as long as their responses are understood and local shelf and harbor resonances are

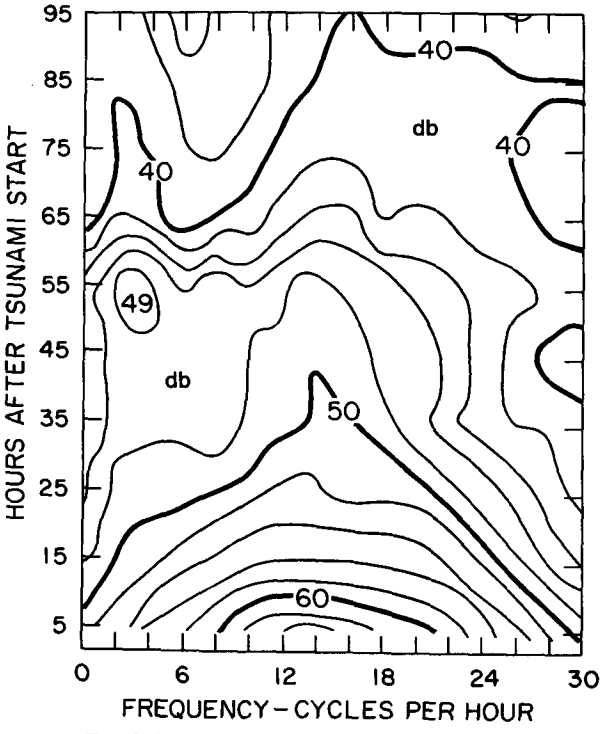

FIG. 9. Energy contours in frequency-time space for tsunami of 9 March 1957 at Wake Island.

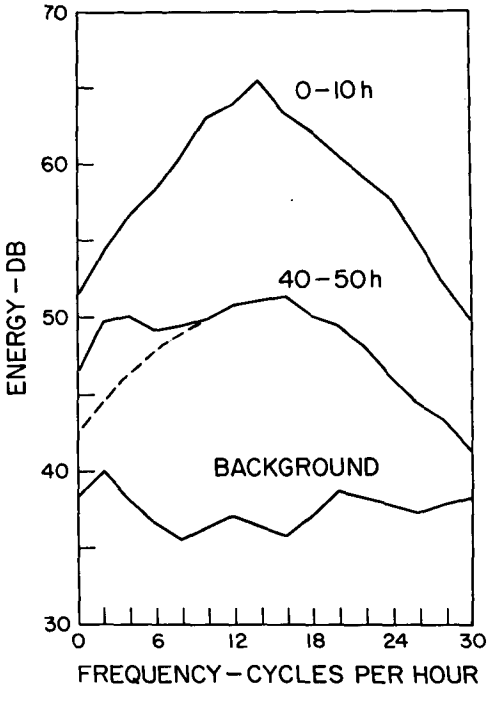

FIG. 10. Power spectra for the tsunami of 9 March 1957 at Wake Island, corrected for instrument and island response.

avoided. As shown below, the background at large island and continental stations is quite different.

c. *Tidegage spectra*

Corresponding sets of spectra to the same resolution (2 cph per estimate) are shown in Figs. 11 and 12 for a matrix of three tsunamis at four tide stations. These twelve spectra are representative of all 28 station events in Table 1. Again there are three curves in each figure, denoting (in descending order) the first 12 hours of the tsunami, the period from 36 to 48 hours and the background. Particular station events will be referred to only by station and date.

The objective in comparing these spectra is to causatively identify common characteristics. For example, background features that prevail at one station can only be environmental since they have nothing to do with tsunamis. Conversely, persistent tsunami features that cannot be identified with background may contain information about source characteristics.

In this context, consider the following background characteristics. To a greater or lesser degree, that at San Diego has an anomalous depression near 11 cph and a broad peak near 16 cph. This is also true for 1952 (not shown) but not for 1946 when the entire background was very low. In three out of four cases where these features exist in the background, they also are present to greater degree in the tsunami spectra. The exception is 1964, already noted for its low-frequency character. Similar features at essentially the same frequencies appear in two of three cases at Honolulu, although only one (1957) is shown in Fig. 12. These relatively high-frequency wiggles are characteristic of small-scale (intra-harbor) resonant responses. Significantly at both San Diego and Honolulu, the response is highest for the 1957 tsunami for which the open-sea spectrum peaked near 14 cph.

As regards tsunamis, distinguishing characteristics are more easily compared at stations where the background spectra are essentially featureless, as at Attu and San Francisco. At both stations the 1957 tsunami spectra are similarly featureless, tending to be richer in mid-frequencies and poorer in low frequencies than corresponding spectra for 1960 and 1964. This type of comparison was optimized by Miller (1972), who minimized the influence of local station response by normalizing early spectra for some twelve different tsunamis at one station to a common base—the November 1952 event. He found these normalized ratios

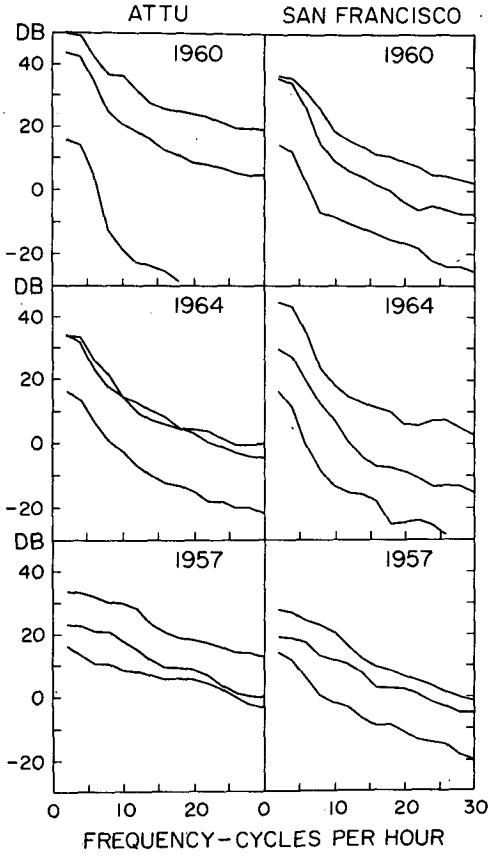

FIG. 11. Comparative power spectra for three tsunamis at two tide stations (see text for details).

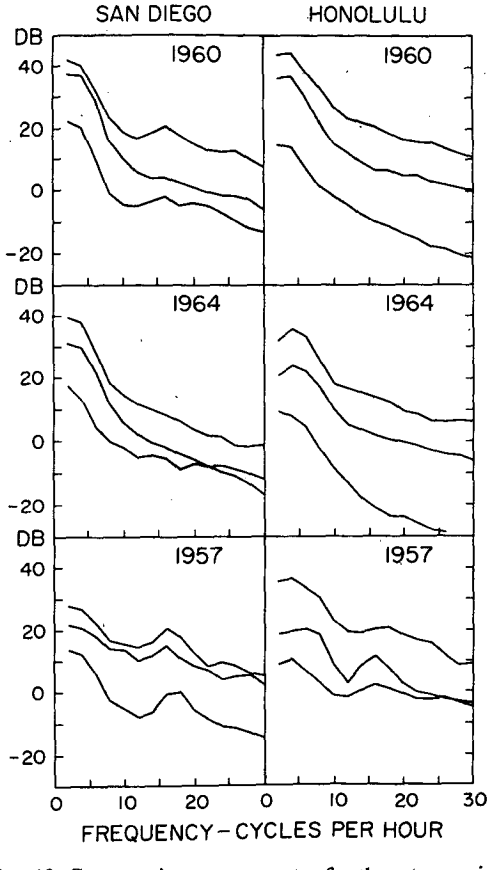

FIG. 12. Comparative power spectra for three tsunamis at two tide stations (see text for details).

to be smooth, monotonic curves with high correlations between stations, from which he concluded that the 1946 and 1957 events were similar and richer in high frequencies than in 1952 and that the converse was true for 1960. But Miller's spectra were computed from 24-hour samples at the beginning of each tsunami and thus were neither directional nor isotropic. A more convincing normalization could be made to the 1957 isotropic tsunami spectrum from Wake Island, i.e., the middle curve in Fig. 9 which should provide estimates of all tsunami spectra in mid-ocean. These normalizations await an optimized island response model now in process and will be reported later. Meanwhile, present results support Miller's conjecture that midocean tsunami spectra are smooth curves and that tidegage responses are dominated by local topographic effects.

In this sense, the remarkable property of the smoothed spectra in Figs. 11 and 12 is not their difference, but their similarity. With few exceptions, the upper (directional) spectrum for each station event could reasonably be reproduced by multiplying the background spectrum by an appropriate factor; the middle (isotropic) spectrum could similarly be obtained using a smaller factor. All spectra are peaked within the range 1–4 cph and are down by 20 db or more by 10 cph. Except for local resonant oscillations, energy above 10 cph was found to degrade roughly as f^{-3}, as previously noted for the Chilean tsunami at La Jolla (Snodgrass *et al.*, 1962).

The above similarities, together with the fact that all tsunamis considered here both originated and were recorded on continental shelves (or large islands) having comparable dimensions, begs the question whether the tsunami signature at a tide gage is principally normal-mode response of the receiving shelf to a directionally-random spectral input, peaked at the frequencies of the transmitting shelf and which manifests itself as a great enhancement of normal background. If so, then the system may be linear, and there is hope of establishing a deterministic model for this behavior. If not, then local response is unique and may be extremely nonlinear; the gage responds similarly—except as to magnitude—no matter what the input, as a bell tied to a bedspring that is remotely shaken. The question cannot be answered on the basis of present evidence, but there are arguments on both sides.

The characteristics of normal background for the simplified case of a straight sloping shelf with parallel contours have been examined in great detail by Munk *et al.* (1964). They found that principal energy was concentrated at frequencies characteristic of the lowest normal "leaky" shelf modes—except for the fundamental (quarter-wave) mode. However, very little energy actually was contained in these modes; instead, most of it was distributed equally among oppositely-traveling, trapped, edge-wave modes at corresponding frequencies. Heuristically, these two types of motion have no causative interactions; practically, it is assumed that they may be coupled through nonlinear interactions such as scattering from contour irregularities. The observed energy distribution was attributed to absence of ambient energy in the open sea at these low frequencies and the probability of it being generated on the shelf by meteorological disturbances.

But this behavior is clearly not characteristic of response to tsunamis. Although weakly-coupled edge waves may well be present, the observed late-stage equilibrium between the ocean and its shelves argues for strong interaction; the abrupt transition from a deep ocean to a shallow shelf argues for energy flux at nearly normal incidence—even from an isotropic ocean; and the high rate of energy dissipation on the shelves (50% per mean reflection) argues for broadened responses and hence, a better impedance match with a broad input spectrum peaked at wavelengths of the same order as the shelf width. Linearity of these processes is evidenced by the fact that the (isotropic) responses to different tsunamis fall in nearly the same ratios at all stations. If one asks why the directive tidegage spectra so resemble the isotropic spectra, the best guess is suggested by Fig. 9. In the open sea, both diffused and directional frequency spectra look alike, although their respective wavenumber spectra do not. Since all frequency information is refracted equally and (almost) normally across the shelf margin, the tidegage responds in the same way to either. But the response magnitude will, in general, be different because the energy transmitted across the shelf by the directional spectrum depends upon its angle of incidence, whereas that for the isotropic spectrum does not.

8. Discussion

As is often the case in research, this study has opened as many doors as it has closed. The concepts and rates of diffusion and isotropic decay of tsunamis seem well established for the northeast Pacific, although one would like confirming evidence from other sectors and from other oceans. The exponential decay rate is much larger than can be accounted for by the usual boundary layer models of fluid mechanics (Stonely, 1964). Since the normal modes of all water bodies decay similarly, one wonders whether some turbulent similarity model might relate these relatively simple geometries. Certainly the decay rate for the Pacific is large enough so that dissipation should be incorporated into numerical tsunami modeling and included in response calculations.

The relative and absolute energies of the five largest tsunamis of this century also seem better defined than previously, although the latter may be improved with a more convincing response model for Wake Island. The door is now open for increased warning reliability, provided that an appropriate sensing station is installed and maintained there. The present tide and tsunami

warning gages at Wake are inadequate for quantitative predictions.

The concept of a linear, one-dimensional, shelf response model—with dissipation included—is being actively pursued. The first test, of course, is to explain the large differences in the responses of individual tidegages to the same (isotropic) input (Table 1). If this steady-state problem can be solved, thus demonstrating that local response is indeed linear, then the early, transient response should be similarly tractable, given the directional input spectrum.

APPENDIX

Tsunami Response at Wake Island

The tsunami of 9 March 1957 was recorded in entirety at a special instrument station on Wake Island, an isolated volcanic atoll in the west-central Pacific (Van Dorn, 1963). This same tsunami, together with those for 1964, 1960 and 1952 (Table 1) were also recorded at the Wake Island tidegage. Thus, a principal objective of the present study was spectral correction of the 1957 *tsunami record (as distinct from tide record)* for island response—the topographic influence of the island on the wave field—leading to an estimate of the spectral distribution of total energy in midocean during the reverberatory decay period.

It was further hoped to cross-correlate the midocean spectra with those computed from the tide record of the same tsunami, thus obtaining a response function that could be applied unambiguously to future tsunamis recorded at Wake. Unfortunately, this latter hope was not realized. All Wake tidal spectra were found to be dominated by a narrow peak near 31 cph, for which the gage response is very nonlinear (Cross, 1968). Rough calculation suggests that this peak is associated with a strong, three-quarter-wave resonance of the small boat harbor in which the tide station is located. This circumstance rendered these invaluable records useless for tsunami analysis.

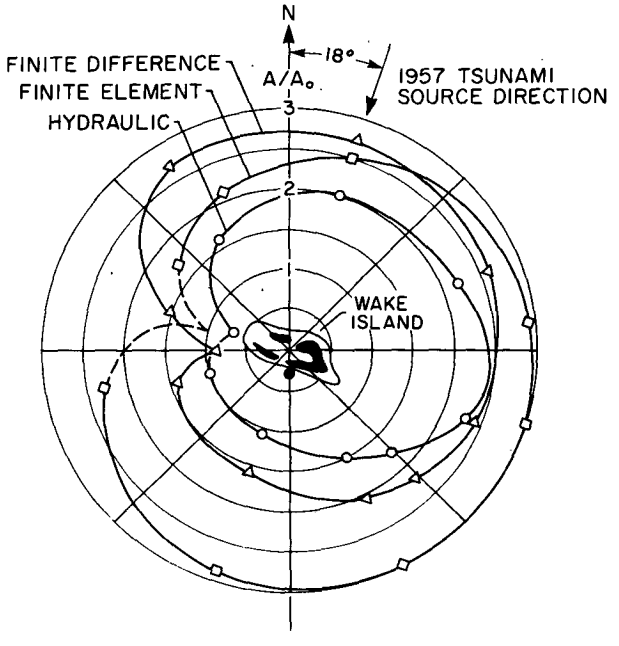

FIG. A1. Comparison of three island response models for plane waves approaching Wake Island from 18° True, as observed at special tsunami station (closed circle).

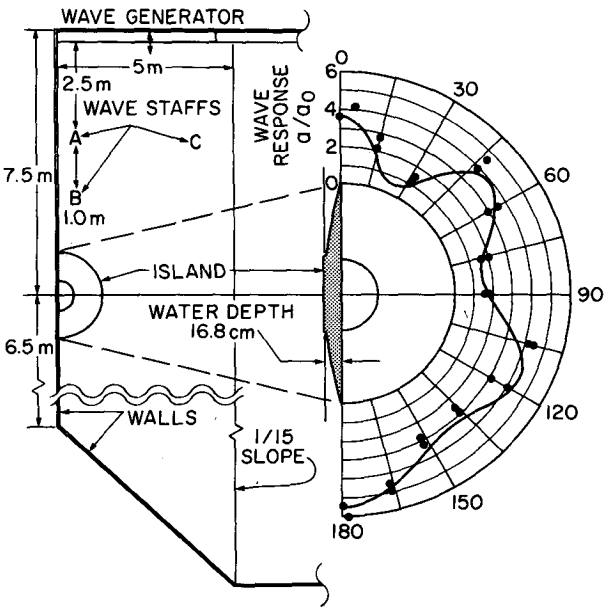

FIG. A2. Polar response plot (right) for hydraulic model test of parabolic half-island model in wave tank (left). Solid curve is theoretical response, dots are data.

The amplitude response of Wake Island was first determined by a hydraulic model experiment (Van Dorn, 1970) and concurrently verified by a numerical finite-difference model (Vastano and Reid, 1970), except that the computed response was larger by about 30%, almost independent of frequency. This discrepancy was jointly ascribed to differences in the assumed boundary conditions. Both experiments were limited to response at selected frequencies to plane waves approaching the island from several directions, as observed from a plurality of points on the island perimeter. Because of the long time lapse, neither experiment was easily reproduced and extended for present purposes.

More recently, Houston (1980) has reported a hybrid finite element method for computing the behavior of dispersive waves in water of finite depth. Because his model was still operational when the present study commenced, he kindly agreed to compute the island response if the input data were supplied. Preliminary calculations showed the finite element response to be again qualitatively similar to that obtained by finite difference but about three times the amplitude. Minor reductions in the shallowest grid-element depths to

make them correspond better to the actual bathymetry on a travel-time basis reduced this disparity by half. Fig. A1 is a polar plot of a "worst case" comparison (wavelength = island circumference at mid-depth) between the hydraulic and the two numerical models for the case of waves from the 1957 tsunami observed at the special recording station. The discrepancy between the two numerical models is still larger than one prefers, especially when similar calculations for a parabolic island for which the response is known analytically gave identical results (Houston, 1980).

In an attempt to resolve this paradox, a parabolic half-island model (scale 1:25 000) was constructed and tested in the 15 m × 20 m wave basin at the Scripps hydraulic facility. Fig. A2 shows the experimental details, together with a polar response plot at the frequency corresponding to ka = (wave number × island radius) = 1.3. The experimental data agree very well with the solid line giving the analytic (and numerical) solution. But Houston's element density adjacent to the parabolic island was about ten times that employed for the Wake model. Thus it seems likely that increasing the element density might result in better agreement between the finite difference and finite element models of Wake. Clearly, it is important to resolve this question, in view of the increasing application of numerical modeling to hydrodynamic problems.

Nevertheless, for present purposes, the island response curve in Fig. 5 was obtained from the finite element model by taking the mean-square amplitude response at the instrument station over all incident directions for each frequency.

REFERENCES

Aida, I., 1978: Reliability of a tsunami source model derived from fault parameters. *J. Phys. Earth,* **26,** 57–73.

Cross, R. H., 1968: Tide gage frequency response. *J. Waterways Harbors Coastal Eng. Div., Amer. Soc. Civ. Eng.,* **94(WW3),** 317–328.

Houston, J. R., 1980: Modeling of short waves using the finite element method. *Proc. Third Int. Conf. on Finite Elements in Water Resources,* University of Mississippi, 5.181–5.195.

Kajiura, K., 1981: Tsunami energy in relation to parameters of the earthquake fault model. *Bull. Earthquake Res. Inst.,* **56,** 415–440.

Loomis, H. G., 1966: Spectral analysis of tsunami records from stations in the Hawaiian islands. *Bull. Seismol. Soc. Amer.,* **56,** 697–713.

Miller, G. R., 1972: Relative spectra of tsunamis. Hawaii Institute of Geophysics Rep. HIG-72-8, University of Hawaii.

——, W. H. Munk and F. E. Snodgrass, 1962: Long-period waves over California's continental borderland. Part II: Tsunamis. *J. Mar. Res.,* **20,** 31–41.

Munk, W. H., 1963: Some comments regarding diffusion and absorption of tsunamis. *Proc. Tsunami Meetings, Tenth Pacific Science Congress,* Honolulu, *IUGG Monogr.,* No. 24, Paris, 53–72.

——, F. Snodgrass and F. Gilbert, 1964: Long waves on the continental shelf: An experiment to separate trapped and leaky modes. *J. Fluid Mech.,* **20,** 529–554.

Ohnaka, M., 1978: Earthquake-source parameters related to magnitude. *Geophys. J. Roy. Astron. Soc.,* **55,** 45–66.

Royer, T. C., and R. O. Reid, 1971: The detection of secondary tsunamis. *Tellus,* **23,** 136–142.

Schureman, P., 1941: *Manual of Tide Observations.* U.S. Dept. Comm. Spec. Pub. No. 196.

Snodgrass, F. E., W. H. Munk and G. R. Miller, 1962: Long-period waves over California's continental borderland. Part I. Background spectra. *J. Mar. Res.,* **20,** 3–30.

Stonley, R., 1964: The propagation of tsunamis. *Geophys. J.,* **8,** 64–81.

Van Dorn, W. G., 1963: The source motion of the tsunami of March 9, 1957 as deduced from wave measurements at Wake Island. *Proc. Tsunami Meetings, Tenth Pacific Science Congress,* Honolulu, *IUGG Monogr.,* No. 24, Paris, 39–48.

——, 1965: Tsunamis. *Advances in Hydroscience,* Vol. 2, Academic Press, 1–48.

——, 1970: Tsunami response at Wake Island: A model study. *J. Mar. Res.,* **28,** 336–344.

——, 1972: A model experiment on the generation of the major tsunami. *The Great Alaska Earthquake of 1964,* Natl. Acad. Sci., 140–146.

Vastano, A. C., and R. O. Reid, 1970: Tsunami response at Wake Island: Comparison of the hydraulic and numerical approaches. *J. Mar. Res.,* **28,** 345–356.